

# A comparison of two methods for state estimation: A statistical Kalman filter, and a deterministic interval-based approach

Nacim Meslem<sup>1</sup> and Nacim Ramdani<sup>2</sup>

**Abstract**—In an uncertain framework the performance of two methods of state estimation for discrete-time linear systems are compared on a pedagogical example. The first one is the well known Kalman filter, which is accurate when the measurement noises and the state disturbances are assumed Gaussian white noises and their statistical properties are available. The second one is a set-membership state estimator, which is also based on the prediction-correction principle. Based on the observability assumption of linear systems combined with interval analysis, both stages of this estimator are carried out in a guaranteed and efficient way. In this study, the performance of both state estimation algorithms are evaluated under two scenarios. In the first scenario, the state disturbances and measurement noise are considered Gaussian and in the second scenario these signals are considered unknown-but-bounded with known bounds.

## I. INTRODUCTION

The aim of this paper is to compare the performance of two types of state estimators dedicated to discrete-time linear systems described by:

$$\begin{cases} \mathbf{x}_{k+1} &= \mathbf{A}\mathbf{x}_k + \mathbf{B}\mathbf{u}_k + \mathbf{d}_k \\ \mathbf{y}_k^m &= \mathbf{C}\mathbf{x}_k + \mathbf{D}\mathbf{u}_k + \mathbf{v}_k \end{cases} \quad (1)$$

where  $\mathbf{x}_k \in \mathbb{R}^n$  is the state vector,  $\mathbf{u}_k \in \mathbb{R}^{n_u}$  is the input vector and  $\mathbf{y}_k^m \in \mathbb{R}^{n_y}$  is the measured output vector. The vectors  $\mathbf{d}_k$  and  $\mathbf{v}_k$  are respectively the state perturbation and the measurement noise, which act on the system. The matrices  $\mathbf{A}$ ,  $\mathbf{B}$ ,  $\mathbf{C}$  and  $\mathbf{D}$  are of appropriate order.

Note that, usually the state disturbances  $\mathbf{d}_k$  and the measurement noises  $\mathbf{v}_k$  are poorly-known and impact the accuracy of the estimated state  $\hat{\mathbf{x}}_k$  of the system (1). Under some assumptions on the nature of these poorly-known signals many state estimation algorithms have been proposed in the literature [9], [16], [6], [1], [12], [7], [13], [11]. In the stochastic context, where these signals are assumed random, independent Gaussian white noises and their statistical properties are well known, the Kalman filter [9] can be efficiently applied. Unfortunately, in general, these assumptions are hard to meet in practice. So, to overcome this restriction set-membership algorithms [6], [4], [1], [10], [2], [3], [5] have been proposed to solve this state estimation problem in a deterministic context. In this context, the state disturbances and the measurement noises are assumed unknown-but-bounded with known bounds. In this work, the performance of the Kalman filter are compared to that of a slightly modified version (an adaptation for the

case of multi-output systems) of the set-membership state estimator introduced in [14]. Both of these estimators are step by step algorithms, where in each step a correction and a prediction procedure is carried out. Two scenarios are considered in this study. The first case: the uncertain parts of the system (1) are assumed Gaussian random variables with well-known statistical properties, namely the mathematical expectations and the covariance matrices. The second case: all the uncertain parts of (1) are assumed unknown but belong to bounded boxes with well-known bounds.

The remainder parts of the paper are organized as follows. To be self-contained, the assumptions and the equations of the Kalman filter are briefly recalled in Section II. Then, a slightly modified version of our interval-based state estimator proposed in [14] is introduced in Section III. Section IV is devoted to evaluate the performance of these two state estimators on a simple example. Stochastic and deterministic contexts are considered to describe the system's uncertainty. Finally, a conclusion on this comparison study is presented in Section V and some works in progress to improve and to extend the application of the proposed interval-based state estimator are indicated.

## II. KALMAN FILTERING

Kalman filter is a state estimator, which alternates between a *correction* and a *prediction* stage. This algorithm uses the probabilistic properties of the state disturbances  $\mathbf{d}_k$ , the measurement noises  $\mathbf{v}_k$  and the initial state  $\mathbf{x}_0$  of the system (1). In this stochastic context, thanks to the Kalman filter, at each time instant  $k$  the random state vector denoted by  $\mathbf{x}_{k|k-1}$  is characterized by an estimation  $\hat{\mathbf{x}}_{k|k-1}$  and a covariance matrix  $\mathbf{G}_{k|k-1}$ .

**Assumption 1:** (i): The vector of the state disturbances  $\mathbf{d}_k$ , the vector of the measurement noises  $\mathbf{v}_k$  and the vector of the unknown initial conditions  $\mathbf{x}_0$  of the system (1) are assumed independent Gaussian white noises. (ii): The mathematical expectations ( $\mathbf{d}_e$ ,  $\mathbf{v}_e$  and  $\mathbf{x}_e$ ) and the covariance matrices ( $\mathbf{G}_d$ ,  $\mathbf{G}_v$  and  $\mathbf{G}_{x_0}$ ) of these random variables are available.

Under this assumption the Kalman equations generate at each time instant  $k$  an estimation  $\hat{\mathbf{x}}_{k|k-1}$  of the state vector  $\mathbf{x}_k$  with a gradually smaller confidence ellipsoid. Note that, this confidence ellipsoid is characterized by the pair  $(\hat{\mathbf{x}}_{k|k-1}, \mathbf{G}_{k|k-1})$ .

a) *Correction:* Notice that, at time instant  $k$  the random state vector  $\mathbf{x}_{k|k}$  is different from that  $\mathbf{x}_{k|k-1}$ . In fact,  $\mathbf{x}_{k|k}$  is characterized when the measurement  $\mathbf{y}_k$  is available. So, the estimation  $\hat{\mathbf{x}}_{k|k}$  and the covariance matrix  $\mathbf{G}_{k|k}$  associated

<sup>1</sup>Nacim Meslem is with Univ. Grenoble Alpes, CNRS, GIPSA-lab, F-38000 Grenoble, France nacim.meslem@gipsa-lab.fr

<sup>2</sup>Nacim Ramdani is with Univ. Orléans, INSA Centre Val de Loire, PRISME, 45000 Orléans, France nacim.ramdani@univ-orleans.fr

to  $\mathbf{x}_{k|k}$  are given by:

$$\begin{aligned} \mathbf{S}_k &= \mathbf{C}\mathbf{G}_{k|k-1}\mathbf{C}^T + \mathbf{G}_v \\ \mathbf{K}_k &= \mathbf{G}_{k|k-1}\mathbf{C}^T\mathbf{S}_k^{-1} \\ \tilde{\mathbf{y}}_k &= \mathbf{y}_k - \mathbf{C}\hat{\mathbf{x}}_{k|k-1} \\ \hat{\mathbf{x}}_{k|k} &= \hat{\mathbf{x}}_{k|k-1} + \mathbf{K}_k\tilde{\mathbf{y}}_k \\ \mathbf{G}_{k|k} &= \mathbf{G}_{k|k-1} - \mathbf{K}_k\mathbf{C}\mathbf{G}_{k|k-1} \end{aligned} \quad (2)$$

b) *Prediction:* Now, the random state vector  $\mathbf{x}_{k+1|k}$  at the time instant  $k+1$  can be characterized by the estimation  $\hat{\mathbf{x}}_{k+1|k}$  and the covariance matrix  $\mathbf{G}_{k+1|k}$  given by:

$$\begin{aligned} \hat{\mathbf{x}}_{k+1|k} &= \mathbf{A}\hat{\mathbf{x}}_{k|k} + \mathbf{B}\mathbf{u}_k \\ \mathbf{G}_{k+1|k} &= \mathbf{A}\mathbf{G}_{k|k}\mathbf{A}^T + \mathbf{G}_d \end{aligned} \quad (3)$$

The graphical interpretation of these estimation results is illustrated in Figure 1. The red cross symbol shows the estimated state vector  $\hat{\mathbf{x}}_{k|k-1}$  and the confidence region with a probability of 0.9 is represented by the magenta ellipsoid. The blue stars stand for some possible values of the state vector at this time instant.

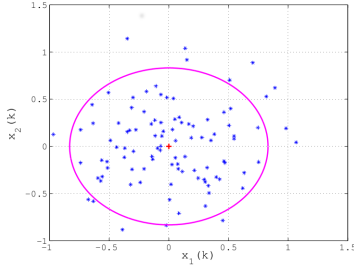


Fig. 1. Graphical description of the state estimation result in the context of the Kalman filter.

Notice that, in [5] a zonotopic Kalman filter is proposed and an explicit bridge between the zonotopic observer and the stochastic Kalman filter is highlighted. In both cases an observer gain has to be designed in order to insure the convergence of the estimation error. On the other hand, in the case of the set-membership state estimator proposed in [14], the convergence of the estimation error is ensured by a set-inversion technique of the collected measurements on a finite-time Horizon.

### III. INTERVAL-BASED SET-MEMBERSHIP STATE ESTIMATOR

Before introducing this set-membership state estimator let us recall some definitions about interval computation [15], [8].

#### A. Interval analysis

A real interval vector (box) of order  $n$  denote by  $[\mathbf{x}]$  is a connected and closed subset of  $\mathbb{R}^n$ , defined as follows:

$$[\mathbf{x}] = [\underline{\mathbf{x}}, \bar{\mathbf{x}}] = \{\mathbf{z} \mid \underline{\mathbf{x}} \leq \mathbf{z} \leq \bar{\mathbf{x}}, \underline{\mathbf{x}}, \bar{\mathbf{x}} \in \mathbb{R}^n\} \quad (4)$$

The real vectors  $\underline{\mathbf{x}}$  and  $\bar{\mathbf{x}}$  are the end-points of the box  $[\mathbf{x}]$  and the inequalities in (4) must be understood element-wise. The set of all interval vectors of  $\mathbb{R}^n$  is denoted by  $\mathbb{IR}^n$ .

Any point of the parallelotope set defined by

$$\mathbb{S} = \{\mathbf{A}\mathbf{x} \mid \mathbf{x} \in [\mathbf{x}]\}$$

where  $\mathbf{A}$  is a real matrix of order  $m \times n$ , can be framed by

$$\mathbf{A}^+\underline{\mathbf{x}} - \mathbf{A}^-\bar{\mathbf{x}} \leq \mathbf{A}\mathbf{x} \leq \mathbf{A}^+\bar{\mathbf{x}} - \mathbf{A}^-\underline{\mathbf{x}} \quad (5)$$

where the entries  $a_{i,j}^+$  of the nonnegative matrix  $\mathbf{A}^+$  are obtained as follows:  $a_{i,j}^+ = \max\{a_{i,j}, 0\}$ ,  $\forall i \in \{1, \dots, m\}$  and  $\forall j \in \{1, \dots, n\}$ . The second nonnegative matrix  $\mathbf{A}^- = \mathbf{A}^+ - \mathbf{A}$ . Note that, the double inequality (5) is useful to implement the interval-based state estimator, which will be presented later.

The width of a scalar interval  $[x]$  is the distance between its end-points

$$w([x]) = \bar{x} - \underline{x} \quad (6)$$

and its midpoint is given by

$$m([x]) = \frac{\bar{x} + \underline{x}}{2} \quad (7)$$

In a similar way, the midpoint of a given box  $[\mathbf{x}] \in \mathbb{IR}^n$  is obtained by

$$M([\mathbf{x}]) = \frac{1}{2}(\bar{\mathbf{x}} + \underline{\mathbf{x}}) \quad (8)$$

and the width of an interval vector  $[\mathbf{x}]$  of order  $n$  is computed as follows:

$$W([\mathbf{x}]) = \max_{i \in \{1, \dots, n\}} \{w([x_i])\} \quad (9)$$

#### B. Interval state estimator

Here, only the knowledge of the end-points of the feasible domains of the uncertain parts of the linear discrete-time system (1) are needed to estimate on-line its state vector. To achieve that, the classical observability property of linear system is used and interval computation are applied.

**Assumption 2:** The feasible domains of the poorly-known variables  $\mathbf{x}_0$ ,  $\mathbf{d}_k$  and  $\mathbf{v}_k$  are bounded with known end-points:

$$\mathbf{x}_0 \in [\underline{\mathbf{x}}_0, \bar{\mathbf{x}}_0] \subset \mathbb{R}^n \quad (10)$$

$$\forall k \geq 0, \begin{cases} \mathbf{d}_k \in [\underline{\mathbf{d}}, \bar{\mathbf{d}}] \subset \mathbb{R}^n \\ \mathbf{v}_k \in [\underline{\mathbf{v}}, \bar{\mathbf{v}}] \subset \mathbb{R}^{n_y} \end{cases} \quad (11)$$

**Assumption 3:** The pair  $(\mathbf{A}, \mathbf{C})$  of the system (1) is observable.

The following algorithm shows the different stages which constitute an interval set-membership state estimator for the uncertain system (1).

**Algorithm: Box-State-Est** $([\mathbf{x}_0], N)$

★★ **Interval-based prediction phase**

- **For**  $k := 1$  to  $k := n - 1$ 
  1.  $[\mathbf{x}_k]_p := \mathbf{A}^k[\mathbf{x}_0] + \mathbf{N}_k \mathbf{1}_n^k[\mathbf{d}] + \sum_{i=0}^{k-1} \mathbf{A}^{(k-i-1)} \mathbf{B}\mathbf{u}_i$
  2.  $[\mathbf{x}_k] := [\mathbf{x}_k]_p$
  3.  $\hat{\mathbf{x}}_k := M([\mathbf{x}_k])$
- **end**

★★ **Interval-based prediction-correction phase**

- **For**  $k \geq n - 1$  to  $N$ 
  4.  $j := k - (n - 1)$   
\*\* *Output set inversion*
  5.  $[\mathbf{x}_j]_{inv} := \mathcal{O}^*([\mathbf{Y}_{(j:j+n-1)}] - \mathcal{O}_d \mathbf{1}_n^{n-1}[\mathbf{d}] - \mathcal{O}_u \mathbf{U}_{(j:j+n-1)})$   
\*\* *Correction at the past time instant  $t_j$*
  6.  $[\mathbf{x}_j]_c := [\mathbf{x}_j]_{inv} \cap [\mathbf{x}_j]_p$   
\*\* *Interval-based prediction stage*
  7.  $[\mathbf{x}_k]_c := \mathbf{M}_1[\mathbf{x}_j]_c + \mathbf{M}_2 \mathbf{1}_n^{n-1}[\mathbf{d}] + \sum_{i=0}^{n-2} \mathbf{A}^{(n-i-2)} \mathbf{B} \mathbf{u}_{j+i}$   
\*\* *Correction at the current time instant  $t_k$*
  8.  $[\mathbf{x}_k] := [\mathbf{x}_k]_c \cap [\mathbf{x}_k]_p$
  9.  $\hat{\mathbf{x}}_k := M([\mathbf{x}_k])$   
\*\* *Go to the next step (time instant  $t_{k+1}$ )*
  10.  $k := k + 1$
  11.  $[\mathbf{x}_k]_p := \mathbf{A}[\mathbf{x}_{k-1}] + \mathbf{B} \mathbf{u}_{k-1} + [\mathbf{d}]$
- **end**
- **Return**  $[\mathbf{x}_k], \hat{\mathbf{x}}_k, k \in \{0, 1, 2, \dots, N\}$

Where  $\mathbf{1}_n^k$  is a concatenation of  $k$  identity matrices of order  $n$ ,

$$\mathbf{1}_n^k = [\mathbf{I}_n \ \mathbf{I}_n \ \dots \ \mathbf{I}_n]^T \quad (12)$$

$$\mathbf{N}_k = [\mathbf{I}_n \ \mathbf{A} \ \dots \ \mathbf{A}^{k-1}] \quad (13)$$

$$\mathbf{M}_2 = [\mathbf{I}_n \ \mathbf{A} \ \dots \ \mathbf{A}^{n-2}] \quad (14)$$

$$\mathbf{M}_1 = \mathbf{A}^{n-1} \quad (15)$$

The matrix  $\mathcal{O}^*$  stands for the generalized inverse matrix of the observability matrix  $\mathcal{O}$

$$\mathcal{O} = \begin{pmatrix} \mathbf{C} \\ \mathbf{CA} \\ \vdots \\ \mathbf{CA}^{n-1} \end{pmatrix}$$

$$\mathcal{O}_d = \begin{pmatrix} \mathbf{0} & \mathbf{0} & \dots & \mathbf{0} \\ \mathbf{CI}_n & \mathbf{0} & \dots & \vdots \\ \vdots & \vdots & \dots & \vdots \\ \mathbf{CA}^{n-2} & \mathbf{CA}^{n-3} & \dots & \mathbf{CI}_n \end{pmatrix}$$

$$\mathcal{O}_u = \begin{pmatrix} \mathbf{D} & \mathbf{0} & \dots & \mathbf{0} & \mathbf{0} \\ \mathbf{CB} & \mathbf{D} & \dots & \vdots & \vdots \\ \vdots & \vdots & \dots & \vdots & \vdots \\ \mathbf{CA}^{n-2}\mathbf{B} & \mathbf{CA}^{n-3}\mathbf{B} & \dots & \mathbf{CB} & \mathbf{D} \end{pmatrix}$$

The real vector  $\mathbf{U}_{(k:k+n-1)}$  gathers a sequence of the system input  $\mathbf{u}_i$  over a finite time-horizon  $i \in \{k, \dots, k+n-1\}$

$$\mathbf{U}_{(k:k+n-1)} = \begin{pmatrix} \mathbf{u}_k \\ \mathbf{u}_{k+1} \\ \vdots \\ \mathbf{u}_{k+n-1} \end{pmatrix}$$

The interval vector  $[\mathbf{Y}_{(k:k+n-1)}]$  is defined as follows:

$$[\mathbf{Y}_{(k:k+n-1)}] = \begin{pmatrix} \mathbf{y}_k^m \\ \mathbf{y}_{k+1}^m \\ \vdots \\ \mathbf{y}_{k+n-1}^m \end{pmatrix} - \mathbf{H}[\mathbf{v}] \quad (16)$$

The real matrix  $\mathbf{H}$  in (16) is obtained as follows:

$$\mathbf{H} = \mathbf{1}_{ny}^n$$

where  $\mathbf{1}_{ny}^n$  is defined in (12).

*c) A brief description:* This algorithm is based on the correction-prediction principle, where the correction stage is applied twice at the current time instant  $k$  and at the past time instant  $j = k - (n - 1)$ .

In the first **For** loop,  $k := 1$  to  $k := n - 1$ , there is not enough measurements to perform the output set-inversion, see the interval equation in line 5. So, for these first iterations the enclosures of the state of the system (1) are computed from the initial state box  $[\mathbf{x}_0]$  by the pre-processing prediction formula used in line 1.

In the second **For** loop,  $k := n - 1$  to  $k := N$ , one has enough measurements to get state enclosures via the output set-inversion formula (line 5). Hence, a first correction of the predicted state enclosure at the past time instant  $t_j$  can be carried out as shown in line 6. Then, from the corrected state enclosure  $[\mathbf{x}_j]_c$ , a new state enclosure  $[\mathbf{x}_k]_c$  of the state of the system (1) at the current time instant  $t_k$  is computed by the pre-processing interval prediction equation described in line 7. In this interval equation the matrices  $\mathbf{M}_1$  and  $\mathbf{M}_2$  are defined in (14)-(15). Finally, a second correction procedure is applied at the current time instant  $t_k$  as illustrated in line 8. For the next step, the predicted state enclosure can be computed directly by the interval extension of (1), see line 11.

**Remark 1:** The multiplications between the real matrices and interval vectors, in the line 1, 5, 7 and 11 of this algorithm, can be performed as suggested in (5).  $\circ$

Figure 2 illustrates graphically the estimation result. The red cross symbol shows the estimated state vector  $\hat{\mathbf{x}}_k$  and the magenta box is the state enclosure of all the possible values of the state vector at the time instant  $k$ . The blue stars stand for some possible values of the state vector at this time instant.

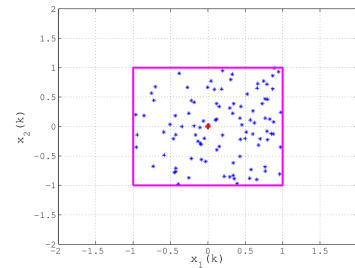


Fig. 2. Graphical description of the state estimation result in the context of the interval-base state estimator.

**Proposition 1:** Under Assumption 2 and 3 the interval algorithm **Box-State-Est** is a set-membership state estimator for the uncertain system (1). Moreover, the width of the estimated state enclosure  $[\mathbf{x}_k]$  is lower than,

$$W([\mathbf{x}_k]) \leq \beta_v W([\mathbf{v}]) + \beta_d W([\mathbf{d}]) \quad (17)$$

after  $n-1$  iterations. Here, the scalars  $\beta_v$  and  $\beta_d$  are defined as follows:

- $\beta_v = \|\mathbf{M}_1\|_\infty \|\mathcal{O}^* \mathbf{H}\|_\infty$  and
- $\beta_d = \|\mathbf{M}_2 \mathbf{1}_n^{n-1}\|_\infty + \|\mathbf{M}_1\|_\infty \|\mathcal{O}^* \mathcal{O}_d \mathbf{1}_n^{n-1}\|_\infty$ .

**Proof.** See the demonstration introduced in our former work [14]. •

**Remark 2:** It is worth pointing out that in this type of state estimator no observer gain is used to ensure the convergence. So, our approach naturally avoids any error amplification induced by the output injection into the dynamics of the interval observers. ◻

The next section is dedicated to compare the performance of these two introduced state estimators on a numerical example. A stochastic and a deterministic context to describe the system's uncertainties are considered.

#### IV. COMPARATIVE STUDY

Consider the following uncertain discrete-time linear system described by

$$\begin{aligned} \mathbf{x}_{k+1} &= \begin{pmatrix} 0.9 & 1 \\ 0 & 0.8 \end{pmatrix} \mathbf{x}_k + \mathbf{d}_k \\ \mathbf{y}_k &= \begin{pmatrix} -22 & 1 \end{pmatrix} \mathbf{x}_k + \mathbf{v}_k \end{aligned} \quad (18)$$

where the feasible domains of the state disturbances, the measurement noise and the initial state of this system are assumed bounded boxes:

$$\begin{aligned} \mathbf{v}_k &\in [-1, 1] \\ \mathbf{d}_k &\in [-1, 1] \times [-1, 1] \\ \mathbf{x}_0 &\in [-10, 10] \times [-10, 10]. \end{aligned} \quad (19)$$

The pair  $(\mathbf{A}, \mathbf{C})$  of this system is observable, then the **Box-State-Est** algorithm can be applied to compute an estimation  $\hat{\mathbf{x}}_k$  of its state vector and its feasible domain  $[\mathbf{x}_k]$ .

##### A. A stochastic context

In this stochastic context the uncertain parts of the system (18) are assumed random Gaussian variables with well-know statistical properties. The numerical values of these properties are gathered in Table I. The random signals  $\mathbf{d}_k$  and  $\mathbf{v}_k$  are generated by the *mvnrnd* MATLAB function and we have selected those which satisfy the two first relationships of (19). The covariance matrix  $\mathbf{G}_{x_0}$  is chosen such that the initial probabilistic confidence ellipsoid, for a probability  $p=0.99$ , is included in the initial box  $[\mathbf{x}_0]$  defined in (19).

TABLE I

THE STATISTICAL PROPERTIES OF  $\mathbf{d}_k$ ,  $\mathbf{v}_k$  AND  $\mathbf{x}_0$ . HERE  $\mathbf{I}_2$  STANDS FOR AN IDENTITY MATRIX OF ORDER 2.

	Mathematical expectation	Covariance matrix
$\mathbf{v}_k$	$\mathbf{v}_e = 0$	$\mathbf{G}_v = 0.12$
$\mathbf{d}_k$	$\mathbf{d}_e = (0, 0)^T$	$\mathbf{G}_d = 0.12 * \mathbf{I}_2$
$\mathbf{x}_0$	$\mathbf{x}_e = (0, 0)^T$	$\mathbf{G}_{x_0} = 10 * \mathbf{I}_2$

Note that, to apply the Kalman filter all these statistical information are necessary. However, the interval-based algorithm, **Box-State-Est**, is based on a less restrictive

assumption, which is the knowledge of the end-points of the feasible domains of the uncertain variables.

The bold black curves in Figure 3 show the enclosures of the system's state variables  $(x_1, x_2)$  provided by the set-membership algorithm, which frames as expected the real state of the system plotted in solid blue lines. These simulation results are obtained with an initial condition of the system (18),  $\mathbf{x}_0 = (5, 5)^T$ . The dashed red curves and the thin green lines show the estimated state variables obtained by the Kalman filter  $\hat{\mathbf{x}}_{k|k-1}$  and the interval-based algorithm  $\hat{\mathbf{x}}_k$ , respectively.

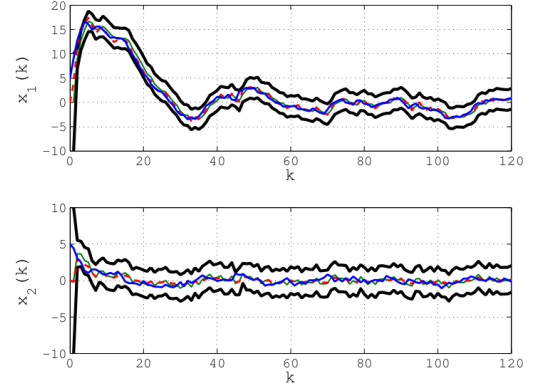


Fig. 3. The estimated state vectors: The continuous blue curves show the evolution of the system's variables. The dashed red lines stand for the estimated state variables provided by the Kalman filter. The dot green lines show the estimated state variables by the interval-based set-membership state estimator. The bold black curves depict the state enclosure computed by the **Box-State-Est** algorithm.

To compare the accuracy of these two estimated state variables, the estimation errors of each case are depicted in Figure 4. The continuous red curves show the estimation error between the state variables of the system and that provided by the Kalman filter  $\mathbf{e}_k = \mathbf{x}_k - \hat{\mathbf{x}}_{k|k-1}$ ; and the dashed blue lines plot the estimation error between the system's state variables and that computed by the interval-based estimator  $\mathbf{e}_k = \mathbf{x}_k - \hat{\mathbf{x}}_k$ . It is clear that, for the first state variable the interval-based estimator is more accurate than the Kalman filter and for the second state variable one gets a similar precision.

The square and ellipsoid sets plotted in the Figure 5 show the feasible domains of the state variables at different time instants  $k$ . The squares are the guaranteed enclosures of the real state vector computed by the interval-based estimator and the ellipsoids are the confidence regions of this state vector provided by the Kalman filter with a probability of 0.9. So, it is clear that the obtained square enclosures are tight and guaranteed to contain the real state vector of the system. However, the Kalman filter cannot claim this guarantee. In term of computation time, the Kalman filter is less demanding. For this simulation the elapsed CPU time is about 0.010s for the Kalman filter case and about 0.018s for the interval-based estimator case (the used CPU is Intel Core i7-3520M CPU 2.90GHz x 4). Note that, the computation time performance of the interval-based algorithm can be

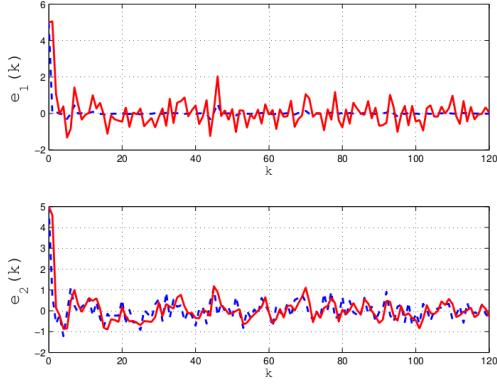


Fig. 4. The evolution of the state estimation error: The red continuous lines represent the difference between the real state variables of the system and that estimated by the Kalman filter. The blue dashed curves shows the gap between the real state variables of the system and that provided by the interval-based set-membership state estimator.

improved by carrying out some steps of this algorithm off-line. This problem will be tackled in forthcoming work.

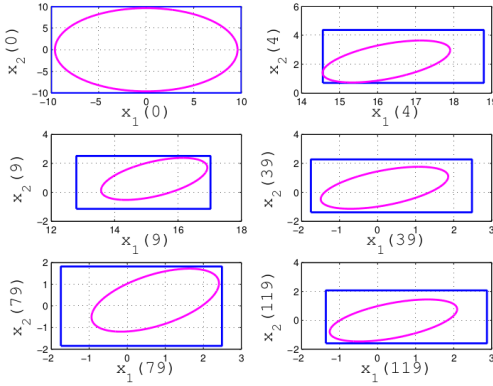


Fig. 5. The feasible sets of the estimated state vectors at the time instants  $k = 0, 4, 9, 39, 79, 119$ . The box sets stand for the guaranteed state enclosures generated by the **Box-State-Est** algorithm. The ellipsoid sets show the probabilistic confidence ellipsoid (here  $p=0.99$ ) estimated by the Kalman filter.

Overall, we can claim that with less information about the system's uncertainties than that needed in the case of Kalman filter, the interval-based estimator provides an accurate estimation of the state vector and characterizes in a guaranteed way its feasible domain.

### B. A deterministic context

Now, we assume that the only available information about the system's uncertainties are the end-points of their feasible domains. Moreover, we assume that the time evolutions of the state disturbances  $\mathbf{d}_k$  and the measurement noise  $\mathbf{v}_k$  are unknown but of a deterministic nature as illustrated in Figure 6.

Notice that, here, the Kalman filter is applied with the same parameters given in Table I. That means, the available information on the evolution of the uncertain signals  $\mathbf{d}_k$  and  $\mathbf{v}_k$  are erroneous. This lack of knowledge of the behavior

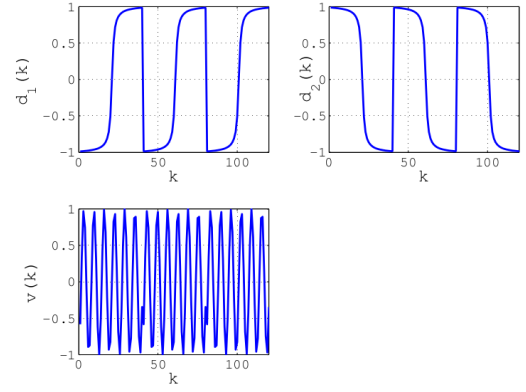


Fig. 6. The time evolutions of the uncertain but deterministic state disturbances and measurement noise.

of these signals has a negative impact on the performance of the Kalman filter. On the other hand, this fact does not disturb the performance of interval-based estimator, because in this case the only required information about the system uncertainties are the end-points of their feasible domains.

The bold black curves in Figure 7 show the state enclosure obtained by the **Box-State-Est** algorithm. This enclosure is tight. As shown in this figure the real state variables of the system (18) (plotted in continuous blue lines) reach the boundaries of this enclosure during some periods of the simulation. However, as observed in this figure the estimated state by the Kalman filter gets out of the guaranteed enclosure at some time instants, for instance at  $k = 1, 41, 81, \dots$

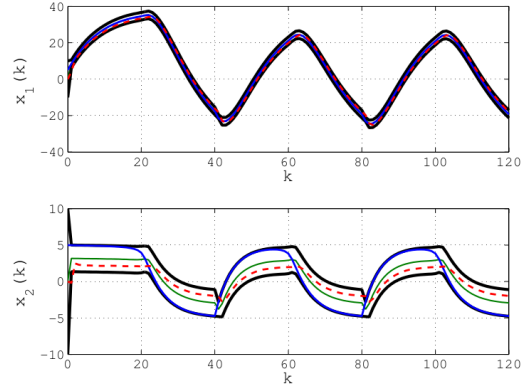


Fig. 7. The estimated state vectors: The continuous blue curves show the evolution of the system's variables. The dashed red lines stand for the estimated state variables provided by the Kalman filter. The dot green lines show the estimated state variables by the interval-based set-membership state estimator. The bold black curves depict the state enclosure computed by the **Box-State-Est** algorithm.

The estimation errors of both cases are depicted in Figure 8. As one can observe, the Kalman estimation error  $\mathbf{e}_k = \mathbf{x}_k - \hat{\mathbf{x}}_{k|k-1}$  is always bigger than that of the interval-based estimator  $\mathbf{e}_k = \mathbf{x}_k - \hat{\mathbf{x}}_k$ .

Figure 9 shows the guaranteed state enclosures and the confidence region of the state vector of the system at



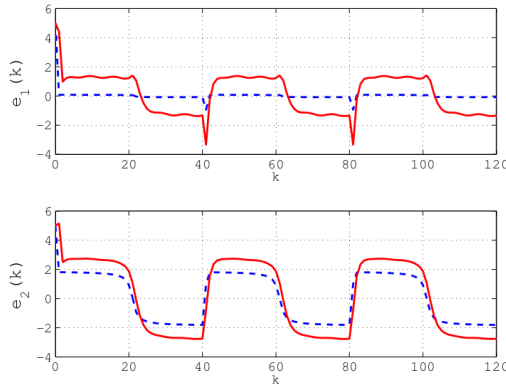


Fig. 8. The evolution of the state estimation error: The red continuous lines represent the difference between the real state variables of the system and that estimated by the Kalman filter. The blue dashed curves shows the gap between the real state variables of the system and that provided by the interval-based set-membership state estimator.

different time instants  $k$ . As we can deduce from these pictures without accurate information about the behavior of state disturbances and the measurement noise, the Kalman filter fails to get guaranteed confidence regions. In fact, as illustrate in Figure 9, the confidence ellipsoids are not completely include in the guaranteed squares generated by the interval-based estimator. Note that, even in this case, the Kalman filter is less demanding in term of the on-line CPU computation time.

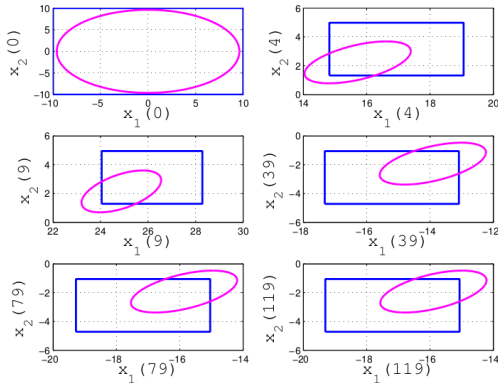


Fig. 9. The feasible sets of the estimated state vectors at the time instants  $k = 0, 4, 9, 39, 79, 119$ . The box sets stand for the guaranteed state enclosures generated by the **Box-State-Est** algorithm. The ellipsoid sets show the probabilistic confidence ellipsoid (here  $p=0.99$ ) estimated by the Kalman filter.

## V. CONCLUSIONS

A comparison between two state estimators for uncertain discrete-time linear systems is presented in this work. The first estimator is based of the statistical properties of the uncertain parts of the system and the second one requires only the knowledge of the end-points of the feasible domains of these uncertain parts. It is shown on a numerical example that when the statistical properties are available the two

estimators provide similar performance. However, in the case where the system's uncertainties can not be described by Gaussian noises and the only available information are the end-points of their feasible domains, the interval-based estimator has better performance than the classical Kalman filter.

In term of on-line computation time, the Kalman filter is less demanding than the interval-based estimator. This issue can be improved in forthcoming work, where certain stages of the interval-based algorithm will be done off-line. Furthermore, in forthcoming work an extension of this interval-based estimator to the case of LTV systems will be proposed.

## ACKNOWLEDGMENT

This work has been partially supported by the LabEx PERSYVAL-Lab (ANR-11-LABX-0025-01).

## REFERENCES

- [1] T. Alamo, J. M. Bravo, and E. F. Camacho. Guaranteed state estimation by zonotopes. *Automatica*, 41:1035–1043, 2005.
- [2] S. Ben Chabane, C. Stoica Maniu, T. Alamo, E. F. Camacho, and D. Dumur. Improved set-membership estimation approach based on zonotopes and ellipsoids. In *Proc. of the IEEE European Control Conference*, pages 993–998, 2014. Strasbourg, France.
- [3] S. Ben Chabane, C. Stoica Maniu, T. Alamo, E. F. Camacho, and D. Dumur. A new approach for guaranteed state estimation. In *Proc. on IFAC World Congress*, pages 6533–6537, 2014. Cape town, South africa.
- [4] C. Combastel. A state bounding observer based on zonotopes. In *Proc. of European Control Conference*, Cambridge, UK, 2003.
- [5] C. Combastel. Zonotopes and kalman observers: Gain optimality under distinct uncertainty paradigms and robust convergence. *Automatica*, 55:265–273, 2015.
- [6] C. Durieu, E. Walter, and B. Polyak. Multi-input multi-output ellipsoidal state bounding. *Journal of Optimization Theory and Applications*, 111(2):273–303, 2001.
- [7] D. Efimov, T. Raissi W. Perruquetti, and A. Zolghadri. On interval observer design for time invariant discrete time systems. *IEEE Conference on European Control Conference, Zurich, Switzerland*, 56(1):266–269, 2013.
- [8] L. Jaulin, M. Kieffer, O. Didrit, and E. Walter. *Applied interval analysis: with examples in parameter and state estimation, robust control and robotics*. Springer-Verlag, London, 2001.
- [9] R.E. Kalman. A new approach to linear filtering and prediction problems. *Transactions of the ASME–Journal of Basic Engineering*, 82(Series D):35–45, 1960.
- [10] V. T. H. Le, C. Stoica, T. Alamo, E. F. Camacho, and D. Dumur. Zonotopic guaranteed state estimation for uncertain systems. *Automatica*, 49(1):3418–3424, 2013.
- [11] N. Loukkas, J.J. Martinez Molina, and N. Meslem. Set-membership observer design based on ellipsoidal invariant sets. In *IFAC, editor, Proceedings of the 19th IFAC World Congress*, Toulouse, France, 2017. IFAC.
- [12] F. Mazenc and S. I. Niculescu T. N. Dinh. Interval observers for discrete-time systems authors. *International journal of robust and nonlinear control*, 24:2867–2890, 2014.
- [13] N. Meslem, N. Loukkas, and J.J. Martinez Molina. A luenberger-like interval observer for a class of uncertain discrete-time systems. In *The 2017 Asian Control Conference*, Gold Coast, Australia, 2017. IEEE.
- [14] N. Meslem and N. Ramdani. Forward-backward set-membership state estimator based on interval analysis. In *The 2018 American Control Conference*, Milwaukee, Wisconsin, USA, 2018. IEEE.
- [15] R. E. Moore. *Interval analysis*. Prentice-Hall, Englewood Cliffs, 1966.
- [16] F. C. Schweppe. Recursive state estimation: Unknown but bounded errors and system inputs. *IEEE Transactions on Automatic Control*, 13(1):22–28, 1968.